CrossMark click for updates

INAUGURAL ARTICLE

SEE COMMENTARY

Plasmodium falciparum evades mosquito immunity by disrupting JNK-mediated apoptosis of invaded midgut cells

Urvashi N. Ramphul, Lindsey S. Garver, Alvaro Molina-Cruz, Gaspar E. Canepa, and Carolina Barillas-Mury[1]

Laboratory of Malaria and Vector Research, National Institute of Allergy and Infectious Diseases, National Institutes of Health, Rockville, MD 20852

This contribution is part of the special series of Inaugural Articles by members of the National Academy of Sciences elected in 2014.

Contributed by Carolina Barillas-Mury, December 10, 2014 (sent for review November 5, 2014; reviewed by George K. Christophides and George Dimopoulos)

The malaria parasite, *Plasmodium*, must survive and develop in the mosquito vector to be successfully transmitted to a new host. The *Plasmodium falciparum Pfs47* gene is critical for malaria transmission. Parasites that express *Pfs47* (*NF54 WT*) evade mosquito immunity and survive, whereas *Pfs47 knockouts* (*KO*) are efficiently eliminated by the complement-like system. Two alternative approaches were used to investigate the mechanism of action of *Pfs47* on immune evasion. First, we examined whether *Pfs47* affected signal transduction pathways mediating mosquito immune responses, and show that the Jun-N-terminal kinase (JNK) pathway is a key mediator of *Anopheles gambiae* antiplasmodial responses to *P. falciparum* infection and that *Pfs47* disrupts JNK signaling. Second, we used microarrays to compare the global transcriptional responses of *A. gambiae* midguts to infection with *WT* and *KO* parasites. The presence of *Pfs47* results in broad and profound changes in gene expression in response to infection that are already evident 12 h postfeeding, but become most prominent at 26 h postfeeding, the time when ookinetes invade the mosquito midgut. Silencing of 15 differentially expressed candidate genes identified caspase-S2 as a key effector of *Plasmodium* elimination in parasites lacking *Pfs47*. We provide experimental evidence that JNK pathway regulates activation of caspases in *Plasmodium*-invaded midgut cells, and that caspase activation is required to trigger midgut epithelial nitration. *Pfs47* alters the cell death pathway of invaded midgut cells by disrupting JNK signaling and prevents the activation of several caspases, resulting in an ineffective nitration response that makes the parasite undetectable by the mosquito complement-like system.

malaria transmission | *Plasmodium* | JNK apoptosis | mosquito immunity | immune evasion

Malaria, a deadly worldwide disease caused by *Plasmodium* parasites, accounts for over half a million deaths annually (1). The mosquito *Anopheles gambiae* is the main vector of human *Plasmodium falciparum* malaria in Africa. The *A. gambiae* midgut is the first tissue infected by *Plasmodium* parasites. Studies using *Plasmodium berghei* (murine malaria) revealed that ookinete invasion irreversibly damages mosquito midgut epithelial cells, leading to cell death (2). Invaded cells activate a two-step nitration response, in which induction of nitric oxide synthase (NOS) (3, 4) is followed by the induction of two other enzymes, heme peroxidase 2 (HPX2) and NADPH oxidase 5 (NOX5), that potentiate nitration (2, 5). When parasites emerge from the basal side of the invaded midgut cell, they come in contact with the complement-like system present in the mosquito hemolymph. The thioester-containing protein 1 (TEP1), a key component of this defense system, binds to the ookinete surface, triggering the formation of a complex that lyses the parasite (6). Nitration reactions modify parasites as they transit through the midgut epithelium, rendering them "visible" to the mosquito complement-like system (5). Induction of HPX2 and NOX5 expression, mediated by the c-Jun-N–terminal kinase (JNK) pathway, is critical to achieve a strong nitration reaction that, in turn, triggers an effective antiplasmodial response by the complement-like system (5, 7, 8).

The JNK pathway is activated when a MAPK kinase (Hemipterous or Hep in *Drosophila*) phosphorylates JNK, which in turn phosphorylates the downstream AP-1 transcription factors, which consist of a Jun and Fos heterodimer (9). Activation of this pathway induces expression of effector genes and of the negative regulator puckered (Puc) (10), a phosphatase that is part of a negative feedback loop that inhibits JNK signaling (11). We have previously shown that disruption of the JNK pathway, by silencing components required for activation, enhanced *P. berghei* infection, whereas overactivation, by silencing the negative regulator Puc, decreased infection (8). JNK-interacting proteins (JIPs) are part of a group of scaffold proteins that help to assemble the JNK pathway components into signaling complexes, thereby enabling JNK activation and signaling (12, 13). In mammals, four JIP proteins that activate the p38 MAPK pathway have been identified, JIP1 (14), JIP2 (15), JIP3 (16, 17), and JIP4 (18), whereas *A. gambiae* has only one JIP gene.

In *Drosophila*, a functional link between JNK signaling and apoptosis has been well established. JNK activates the transcription factors forkhead box O (FOXO) and *Fos*, that in turn activate *Hid* expression (19). FOXO is part of a family of transcription factors that is phosphorylated by Akt or IKK in response to signals promoting survival (19). However, lack of these

Significance

The *Anopheles gambiae* mosquito is a very effective vector of human *Plasmodium falciparum* malaria. We recently found that the *Pfs47* gene allows the parasite to survive, by evading the mosquito immune system. In this study, we explored the mechanism of *Pfs47* immune evasion. We found that *Pfs47* inhibits Jun-N-terminal kinase-mediated activation of apoptosis in invaded mosquito midgut cells by preventing activation of several caspases. Furthermore, the lack of caspase-S2 activation prevents the induction of enzymes that potentiate epithelial nitration, a reaction required for parasites to be "visible" to the mosquito complement-like system. These findings shed new light on how a single parasite gene inactivates the mosquito immune system and allows it to be successfully transmitted to a new host.

Author contributions: U.N.R., L.S.G., and C.B.-M. designed research; U.N.R., L.S.G., A.M.-C., and G.E.C. performed research; U.N.R. and C.B.-M. analyzed data; and U.N.R. and C.B.-M. wrote the paper.

Reviewers: G.K.C., Imperial College London; and G.D., Johns Hopkins University.

The authors declare no conflict of interest.

Freely available online through the PNAS open access option.

See Profile on page 1245.

See Commentary on page 1250.

[1]To whom correspondence should be addressed. Email: cbarillas@niaid.nih.gov.

This article contains supporting information online at www.pnas.org/lookup/suppl/doi:10.1073/pnas.1423586112/-/DCSupplemental.

MICROBIOLOGY

survival signals results in FOXO translocating to the nucleus from the cytoplasm and inducing apoptosis (19, 20). Recently, it was reported that low levels of insulin-like growth factor 1 in human blood induced midgut FOXO activation, resulting in increased *Anopheles stephensi* lifespan (21).

In *Drosophila*, inhibitors of apoptosis (IAPs) and IAP antagonists, such as head involution defective (hid), reaper, and grim, play an important role in regulating cell death (22). Head involution-defective (*Hid*) activates the initiator caspases *Dredd* and *Dronc* by suppressing the activity of *Drosophila* inhibitor of Apoptosis 1 (*Diap1*) (23, 24). Caspases are cysteinyl aspartate proteinases (Cys-proteases) that cleave peptides after Asp residues and can trigger apoptosis (25). Initiator caspases contain long prodomains and activate effector caspases containing short prodomains involved in cleavage of downstream substrates required for disassembly (26, 27).

Other immune signaling cascades, such as the immune deficiency (IMD), Toll, and JAK/STAT pathways, have also been implicated in antiplasmodial responses in the mosquito (28–31). For example, activation of the Toll pathway is more effective against the rodent malaria parasite, *P. berghei* (28), whereas the IMD pathway is more effective against the human malaria parasite, *P. falciparum* (30). Disruption of IMD signaling enhances *P. falciparum* infection, whereas overactivation of this pathway, by silencing the negative regulator Caspar, greatly reduces infection (30, 31). The STAT pathway, in turn, mediates late-phase immune responses that target early oocysts through a TEP1-independent mechanism (32).

Recent studies revealed that the *P. falciparum Pfs47* gene is critical for malaria transmission, because it allows the parasite to evade the *A. gambiae* complement-like system and escape unharmed (33). Wild-type (*WT*) *P. falciparum NF54* parasites effectively evade the *A. gambiae* immune system, and *Pfs47 knockout* (*KO*) parasites (*NF54* background) are efficiently eliminated by the mosquito complement-like system (33). Silencing TEP1 had no significant effect on the intensity or prevalence of infection with *NF54 WT*, indicating that this defense system was not actively limiting parasite survival. In contrast, reducing TEP1 expression had a dramatic effect on infections with the *Pfs47 KO* line, greatly increasing parasite survival (33). The presence of *Pfs47* suppresses the midgut nitration responses (33), a critical step needed to activate TEP1-mediated lysis (5). *NF54 WT* parasites expressing *Pfs47* did not induce HPX2 and NOX5 expression when they invaded the midgut, and nitration levels were even lower than in uninfected controls; however, *Pfs47 KO* parasites triggered high induction of HPX2 and NOX5, resulting in a strong nitration response (33).

In this study, we used two different approaches to investigate the mechanism of action of *Pfs47* on immune evasion in the mosquito. First, we examined whether *Pfs47* affects some of the *A. gambiae* signal transduction pathways known to regulate TEP1-mediated antiplasmodial immune responses. Because the JNK pathway mediates midgut nitration in response to *P. berghei* infection, and epithelial nitration responses are inhibited in *P. falciparum NF54* parasites expressing *Pfs47*, we investigated the hypothesis that *Pfs47* prevents nitration by disrupting JNK signaling. Based on previous work that has shown that the IMD pathway limits infection with *NF54 WT* parasites (31), we also investigated whether this pathway is active in the absence of *Pfs47*. Second, we undertook a broad approach, using microarrays to compare the genome-wide transcriptional responses of the mosquito midgut to infections with wild-type and *Pfs47 KO P. falciparum*. The potential participation of several differentially expressed genes, representing novel effector candidate genes, was evaluated by exploring the effect of silencing them on *Plasmodium* survival. These studies uncovered a broad effect of *Pfs47* on midgut epithelial responses to invasion.

Results

The JNK Pathway Is a Key Mediator of *A. gambiae* Antiplasmodial Responses to *P. falciparum* Infection That Is Disrupted by *Pfs47*. To investigate whether *Pfs47* affects the JNK pathway, we first assessed the effect of activating or suppressing JNK signaling on infections with *NF54 WT* parasites. Either disruption of this cascade, by silencing JIP1, JNK, Fos, or Jun, or overactivation by silencing the suppressor Puc, had no effect on either the intensity or prevalence of infection (Fig. 1), indicating that the JNK pathway is not actively limiting infection in *NF54* parasites that express *Pfs47*. Because the JNK pathway regulates HPX2 and NOX5 expression (8), our results agree with the previous observation that expression of these two enzymes is not induced in midguts infected with *NF54 WT* parasites (33).

To determine whether the lack of response to JNK signaling was caused by *Pfs47*, we silenced the same JNK pathway components in mosquitoes infected with *Pfs47 KO* parasites. Here, silencing JIP1 ($P = 0.0034$), JNK ($P = 0.0011$), Fos ($P = 0.0051$), or Jun ($P = 0.0004$) significantly enhanced both the intensity and prevalence of infection (Fig. 2). Not surprisingly, silencing Puc had the opposite effect, reducing the infection intensity ($P = 0.0220$) and infection prevalence from 66–39% ($P = 0.0121$). Taken together, these findings indicate that the JNK pathway mediates a robust immune response to *P. falciparum* infection that is no longer triggered by parasites expressing *Pfs47*. This finding is also consistent with the previous observation that HPX2 and NOX5 expression are highly induced, and nitration levels are high in mosquito midguts infected with *Pfs47 KO* parasites (33).

Previous work has shown that overactivating the IMD pathway by silencing Caspar, a negative regulator, confers protection from infection with *NF54* parasites in *A. gambiae*, *A. stephensi*, and *Anopheles albimanus* (30, 31, 34). Furthermore, introducing extra copies of Rel2, a key transcription factor of the IMD pathway, in *A. stephensi* also reduced infection (34). Here, silencing the IMD receptor increased infection with both *NF54 WT* ($P = 0.0449$) and *Pfs47 KO* parasites ($P = 0.0017$) (Fig. S1 *A* and *B*). This finding confirms the role of the IMD pathway in limiting *P. falciparum NF54 WT* infection, as previously described (31), and indicates that activation of this pathway is not affected by *Pfs47*.

In *Drosophila*, the kinase TAK1 (transforming growth factor β-activated kinase 1) is capable of activating both JNK and IKK (and NF-κB signaling) after immune stimulation (35). TAK1 has been proposed as a possible link that activates both the IMD and JNK pathways (36–38). However, previous work has shown no protective role of TAK1 against *P. falciparum NF54 WT* in *A. gambiae* (31). Here, silencing TAK1 also had no effect on *Pfs47 KO* infection intensity or prevalence, indicating that this gene is not essential to limit *P. falciparum* infection (Fig. S1*C*).

Midgut Transcriptional Responses to *Plasmodium* Infection. We compared the midgut transcriptional response to infection with *NF54 WT* or *Pfs47 KO P. falciparum* parasites using microarrays, to better understand the effect of *Pfs47* on the epithelial response to infection. The transcriptome of female mosquitoes fed uninfected blood was used as reference to establish the responses that were a result of blood feeding. Midguts were collected at 12 h postfeeding (PF) (before invasion) and at 26 h PF, the time when ookinetes are invading the midgut epithelium. The expression of a subset of 12 genes was validated by real-time quantitative PCR (qRT-PCR) to assess the accuracy of the microarray data (Fig. S2*A*). The correlation between the microarray and qRT-PCR results was high (Pearson correlation coefficient $R^2 = 0.9237$) and highly significant ($P < 0.0001$), validating the microarray mRNA expression data.

We first analyzed the overall midgut transcriptional responses at 12 h PF. At this time, the number of genes significantly

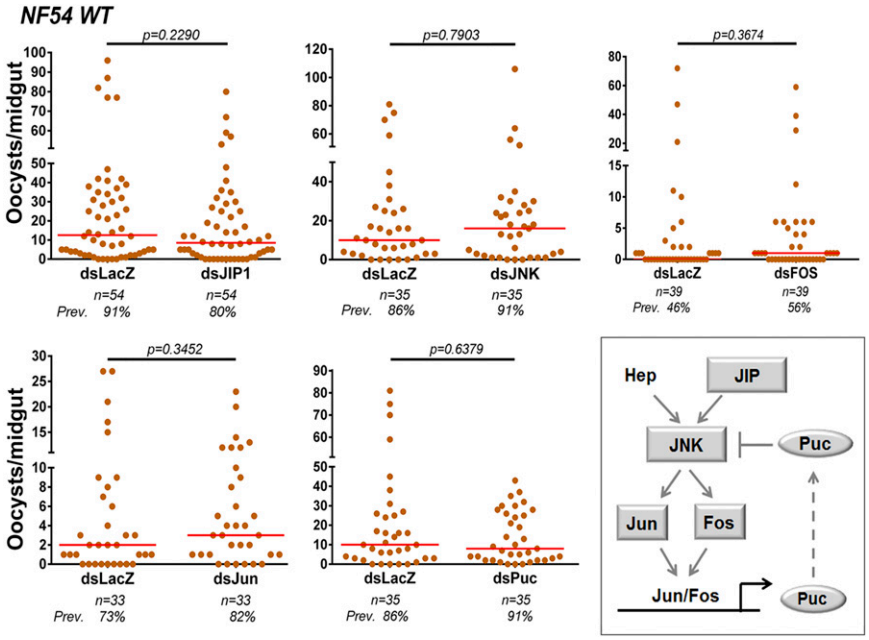

Fig. 1. Effect of silencing JNK pathway components on *NF54 WT* infections. Effect of silencing JIP1, JNK, Fos, Jun, and Puc on *NF54 WT* infection 7–10 d PF. Orange dots represent oocyst counts from individual mosquito midguts and medians are represented by red lines. Each phenotype was confirmed with two to three independent experiments. (*Inset*) *A. gambiae* orthologs of the *Drosophila* JNK signaling cascade. Geometric shapes represent genes phenotyped using RNAi. Gray color indicates that silencing had no significant effect on infection intensity.

induced with equal or greater than twofold (1.0 in $\log_2$ scale) change by *NF54 WT* (578), relative to uninfected controls, were 3.5-times higher than the number of induced genes by *Pfs47 KO* parasites (164), indicating that the presence of *Pfs47* in zygotes or immature ookinetes triggers the induction of a large number of genes (Fig. 3*A*). A similar number of genes were suppressed in response to infection with *NF54 WT* or *Pfs47 KO* parasites. As shown in the Venn diagram, the proportion of individual genes that had a similar response, and were either induced or suppressed in response to infection with both *NF54 WT* and *Pfs47 KO* parasites, represent only 10% and 16%, respectively, of the total number of genes with significant changes in expression relative to uninfected controls (Fig. 3*A*). Some drastic differences in gene expression (3.02- to 91.5-fold) (Fig. S2*C*) between mosquitoes infected with *WT* and *KO* parasites were observed at this early time. The three most prominent groups of induced genes were serine proteases, odorant binding proteins, and cuticular proteins (Fig. S2*C* and Table S1). Several of the proteases belonged to the CLIP family, suggesting that they may be involved in cell signaling rather than blood digestion. The complete list of genes with a difference in expression threefold or higher is shown in Table S1.

At the time when ookinetes are invading the mosquito midgut (26 h PF), a comparable number of genes were transcriptionally induced (656 genes) and suppressed (652 genes) in response to infection with *NF54 WT* parasites (Fig. 3*B*). However, a striking difference was observed in *Pfs47 KO*-infected midguts, in which the number of suppressed genes (1,004) was 2.7-times higher than the number of induced genes (378) (Fig. 3*B*). Interestingly, the genes suppressed belong to a broad range of functional

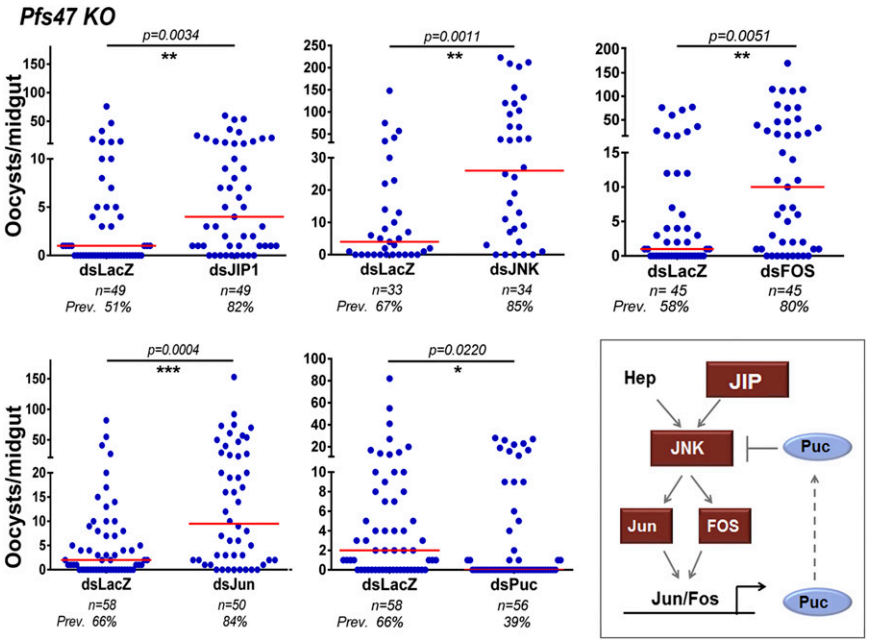

Fig. 2. Effect of silencing JNK pathway components on *Pfs47 KO* infections. Effect of silencing JIP1, JNK, Fos, Jun, and Puc on *Pfs47 KO* infection 7–10 d PF. Blue dots represent number of oocysts from an individual midgut and red lines represent medians. All graphs represent two to three independent biological replicates. (*Inset*) *A. gambiae* orthologs of the *Drosophila* JNK signaling cascade. Geometric shapes represent genes phenotyped using RNAi. Red indicates that silencing significantly increased infection intensity and blue represents a significant decrease in infection intensity.

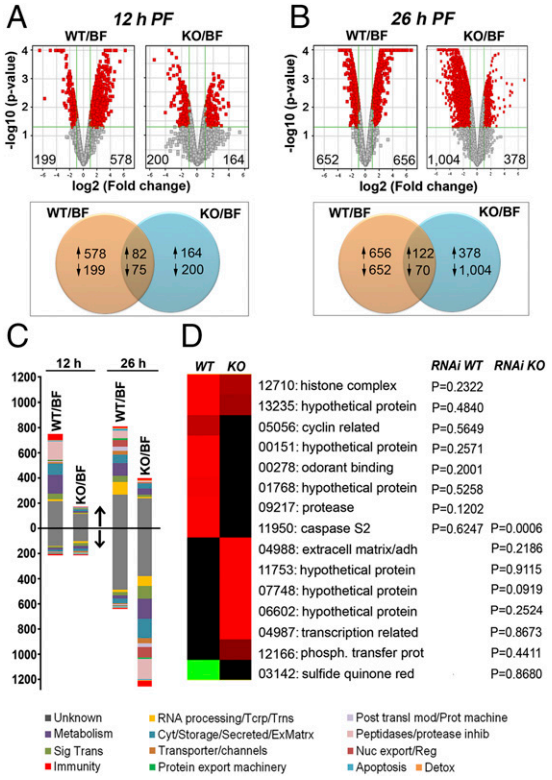

Fig. 3. Transcriptional responses of the mosquito midgut to *NF54 WT* or *Pfs47 KO* infection and gene expression patterns. (*A*) Volcano plots and Venn diagrams showing the number of induced and suppressed genes with two-fold change (1.0 in $\log_2$ scale) or higher (in red) in midguts infected with *NF54 WT* relative to bloodfed (BF) control and *Pfs47 KO* relative to BF control at 12 h PF or (*B*) 26 h PF. Venn diagrams indicate the number of individual genes induced or suppressed in response to infection with either or both parasite strains. (*C*) Proportion of differentially regulated genes according to functional classes which are either up- or down-regulated at the two time points at 12 and 26 h PF. Functional classes of induced genes are represented above the horizontal black line and suppressed genes are below the line (indicated by arrows). (*D*) Expression profiles of candidate genes with strong differences in expression (5- to 103.78-fold) that were selected for phenotypic analysis by RNAi. The corresponding *P* values (Mann–Whitney) were obtained after gene silencing and following infection with either *NF54 WT* or *Pfs47 KO* are listed, relative to dsLacZ control. The last five numbers of AGAP IDs are shown (e.g., 12710 = AGAP012710). Cyt/storage/secreted/ExMatrx: Cytoskeletal/Storage/Secreted/Extracellular Matrix; Imm: immunity; Met: metabolism; Nuc export/Reg: nuclear export and regulation; Phosph. transfer protein: phosphatidylinositol transfer protein; RNA processing/Tcrp/Trns: RNA processing, transcription, translation; Sig Trans: signal transduction; sulfide quinone red: sulfide quinone reductase; St: signal transduction; Unk: unknown.. AGAP009217 and AGAP003142 were differentially expressed at 12 h PF; AGAP013235, AGAP011950, AGAP011753. and AGAP000278 at both 12 and 26 h PF; and all other genes exhibited differential expression at 26 h PF.

classes, such as proteases, secretion/storage, metabolism, and signal transduction (Fig. 3*C*). Because only a small proportion of cells are typically invaded by *Plasmodium* parasites, the large number of suppressed genes by *Pfs47 KO* parasites suggests that invaded cells, and most likely also neighboring cells, suppress several basic metabolic functions. The proportion of genes that had a common response to infection with *NF54 WT* or *Pfs47 KO* at 26 h PF was minimal, consisting of 11% up-regulated and 4% down-regulated genes, highlighting the profound effect of *Pfs47* on the midgut response to infection.

We selected 15 candidate genes that were strongly induced (5- to 103.78-fold) in response to infection with one parasite line, but not the other (Fig. 3*D*), and evaluated the effect of silencing expression on the level of infection with the parasite line that triggered a higher level of mRNA expression. Silencing most genes (14 of 15) had no effect on the level of infection, relative to the LacZ control (Fig. S3). However, silencing caspase S2 (CASP-S2) significantly increased the intensity of infection with *Pfs47 KO* parasites ($P < 0.0006$), but had no effect on *NF54 WT* parasites (Fig. 3*D*), indicating that *Pfs47* may be affecting the mechanism of cell death in *Plasmodium*-invaded midgut cells.

Enhancing the Sensitivity of Double-Stranded RNA-Mediated Silencing in *P. falciparum* Infection Screens. The original silencing protocols were optimized for *P. berghei* infections, in which infected mosquitoes are kept at 19–20 °C, a permissive temperature for parasite development. We reasoned that the mosquito epithelial responses to ookinete invasion would be much faster when they are infected with *P. falciparum* and kept at 26 °C. We were concerned that the lack of phenotype in 14 of the 15 target genes silenced could be because of lack of sensitivity in the screen. For example, when silencing genes coding for enzymes, the residual catalytic activity would be much higher at 26 °C and this could mask the phenotype. We first evaluated the effect on parasite survival of slowing down the epithelial responses by reducing the temperature of *P. falciparum*-infected mosquitoes from 26 °C to 22 °C between 6 and 36 h PF on the infectivity of the parasite. This temperature switch, at the critical time of ookinete maturation and midgut invasion, had no significant effect on the intensity ($P = 0.7632$) or prevalence ($P = 0.3330$) of infection (Fig. S4*A*). However, as expected, the effect of silencing several genes on survival of *Pfs47 KO P. falciparum* parasites was stronger when the temperature was reduced for genes such as IMD (the level of significance went from $P < 0.0029$ to $P < 0.0007$) (Fig. S4*B*), and for two hypothetical proteins of unknown function, AGAP006602 (from $P < 0.2524$ to $P < 0.0210$) and AGAP007748 (from $P < 0.0919$ to $P < 0.0037$) (Fig. S4*C*). These data indicate that the transient temperature switch increases the sensitivity of screens involving double stranded RNA (dsRNA)-mediated gene silencing, so this protocol was used in all subsequent experiments. The kinetics of ookinete invasion under this experimental set-up was also evaluated by measuring the changes in expression of Serpin 6 (SRPN6) mRNA, a gene highly induced in response to *Plasmodium* infection and a very sensitive marker of midgut invasion (39), at 24 and 28 h PF (Fig. S4*D*). SRPN6 expression was the same in midguts of mosquitoes fed uninfected blood or infected with *Pfs47 KO* parasites at 24 h PF, but at 28 h PF, SRPN6 expression was highly induced in the infected group, indicating that ookinete midgut invasion was taking place at this later time point.

Caspases Limit Mosquito Infection with *P. falciparum* Parasites That Lack *Pfs47*. There are four IAPs in *Drosophila*, but in *A. gambiae* this gene family has expanded. Four of the seven mosquito genes appear to cluster with *Drosophila* IAP1, but a clear ortholog of *Dm* IAP1 cannot be defined. Here, we focused on *A. gambiae* IAP1 (AGAP007294) because its putative ortholog in the mosquito *Aedes aegypti* has been implicated in regulation of apoptosis (40). Putative orthologs of *Dredd* and *Dronc* are present in *A. gambiae* (Fig. S5 *A* and *B*). We investigated whether the observed differences in JNK signaling between *NF54 WT* and *Pfs47 KO* parasites affect activation of the *A. gambiae* initiator caspases L1 (CASP-L1) and L2 (CASP-L2), orthologs of *Drosophila Dredd* and *Dronc*, respectively (Fig. S5 *A* and *B*).

In *Drosophila*, *Dredd* and *Dronc* activate five effector caspases (Fig. S5*C*), but in *A. gambiae* the number of effector caspases has expanded to 14 genes (Fig. S5*D*). Although there are no 1:1 orthologs between *Drosophila* and *A. gambiae*, effector caspases cluster into three homologous groups in both species (Fig. S5 *C* and *D*). We determined the expression levels of the transcription factor FOXO, and of initiator and effector caspases 28 h PF and found that FOXO and CAPSP-L1 expression are induced in

response to infection with *Pfs47 KO*, but not with *NF54 WT* parasites (Fig. S6*A*). We proceeded to silence FOXO, IAP1, the initiator caspases (CASP-L1 and CASP-L2), as well as those effector caspases with strong transcriptional responses following infection with either *NF54 WT* or *Pfs47 KO* parasites (CASP-S2, -S3, -S4, -S5, -S6, -S8, and -S10) (Fig. S6*A*).

Silencing the initiator caspases, CASP-L1 (Fig. 4*A*), CASP-L2 (Fig. S6*B*), or IAP1 (Fig. S6*C*) resulted in no significant change in infection intensity ($P = 0.8496$, $P = 0.8903$, and $P = 0.6070$, respectively) or infection prevalence ($P = 0.5577$, $P = 0.6098$, and $P = 1.000$, respectively) in mosquitoes infected with *NF54 WT* parasites. However, silencing FOXO significantly decreased oocyst numbers ($P = 0.0078$) and the prevalence of infection from 99–81% ($P = 0.0019$) (Fig. 4*A*).

Silencing FOXO or CASP-L1 significantly increased the number of developing *Pfs47 KO* oocysts ($P = 0.0006$ and $P = 0.0086$, respectively) and prevalence of infection from 36–74% ($P = 0.0001$) and 38–69% ($P = 0.0111$), respectively (Fig. 5*A*), whereas silencing IAP1 or CASP-L2 had no effect on oocyst numbers or infection prevalence (Fig. S6 *B* and *C*). This finding indicates that midgut invasion of parasites lacking *Pfs47* activates an apoptotic response involving FOXO and CASP-L1 that is very effective in limiting infection, whereas in the presence of *Pfs47*, this pathway does not limit parasite survival.

Silencing the effector caspases CASP-S3, CASP-S4, CASP-S5, CASP-S6, and CASP-S10 had no effect on infection intensity or prevalence on *NF54 WT* parasites, but silencing CASP-S8 significantly decreased intensity of infection ($P = 0.0051$) and the prevalence of infection from 99–86% ($P = 0.0094$) (Fig. 4 and Fig. S7*A*). In contrast, silencing these effector caspases enhanced *Pfs47 KO* infection (Fig. 5 and Fig. S7*B*), CASP-S3 ($P = 0.0010$), CASP-S4 ($P = 0.0006$), CASP-S5 ($P = 0.0149$), CASP-S6 ($P = 0.0106$), and CASP-S8 ($P = 0.0016$), with the exception of CASP-S10, which had no effect ($P = 0.7527$). The most striking phenotypic differences observed were the effect of silencing FOXO and CASP-S8, which reduced infection of *NF54 WT* parasites, but enhanced infection of the *Pfs47 KO* strain (Figs. 4 and 5 and Fig. S7), and of silencing CASP-S2 and CASP-S4, which had no effect on *NF54 WT* infection (Fig. 4*B* and Fig. S7*A*) but resulted in a robust increase in infection intensity of *Pfs47 KO* parasites, increasing the median number of oocysts from 2 to 16 ($P = 0.0006$) and 1–8.5 ($P = 0.0006$) and prevalence of infection from 54–90% ($P < 0.0001$) and 59–81% ($P = 0.0115$), respectively (Fig. 5*B* and Fig. S7*B*). All effector caspases but one (CASP-S10) enhanced infection with *Pfs47 KO* parasites, suggesting that the presence or lack of *Pfs47* is central in determining whether caspases are activated and induce apoptosis. Taken together, these gene-silencing experiments demonstrate that a single parasite gene, *Pfs47*, can drastically alter the cell-death pathway of invaded midgut cells by disrupting JNK signaling and preventing the activation of the initiator caspase CASP-L1 and of several downstream effector caspases.

The JNK Pathway Regulates Activation of Caspases and Epithelial Nitration in Invaded Midgut Cells. The JNK pathway is known to regulate apoptosis in *Drosophila* (10) and has also been shown to activate caspases in human cell lines (41). We obtained direct evidence that infection with *Pfs47 KO* parasites, in which JNK signaling limits parasite survival, induces activation of caspase activity (Fig. 6*A*) that is significantly higher than with *NF54 WT* parasites (Fig. 6*A*, *Left*). Furthermore, disruption of JNK signaling by silencing JNK significantly reduces the induction of caspase activity in midguts infected with *Pfs47 KO* parasites, indicating that JNK signaling is required to activate caspase-mediated apoptosis of *Plasmodium*-invaded midgut cells (Fig. 6*A*, *Right*).

Previous studies have shown that JNK signaling activates the induction of NOX5 and HPX2, two enzymes that potentiate midgut nitration and are required to trigger an effective activation of the mosquito complement-like system (5). Infection with *Pfs47* KO parasites induces the expression of these two enzymes and a robust nitration response that is not observed in midguts infected with *NF54 WT* parasites (33). Silencing CASP-S2 prevented the induction of NOX5 and HPX2 expression (Fig. 6*B*), indicating that the regulation of these midgut enzymes that potentiate nitration by the JNK pathway requires activation of CASP-S2.

Discussion

In this study, we carried out several functional assays to explore how *Pfs47* affects mosquito epithelial responses to parasite invasion to evade immunity. We found that the JNK pathway is not effective in limiting infection in mosquito midguts invaded by *NF54 WT* parasites that express *Pfs47*, as silencing multiple components required for signaling activation had no effect on infection intensity or prevalence. Furthermore, *Pfs47* appears to actively suppress JNK signaling, as it was also not possible to activate this cascade by silencing the suppressor puckered (*Puc*).

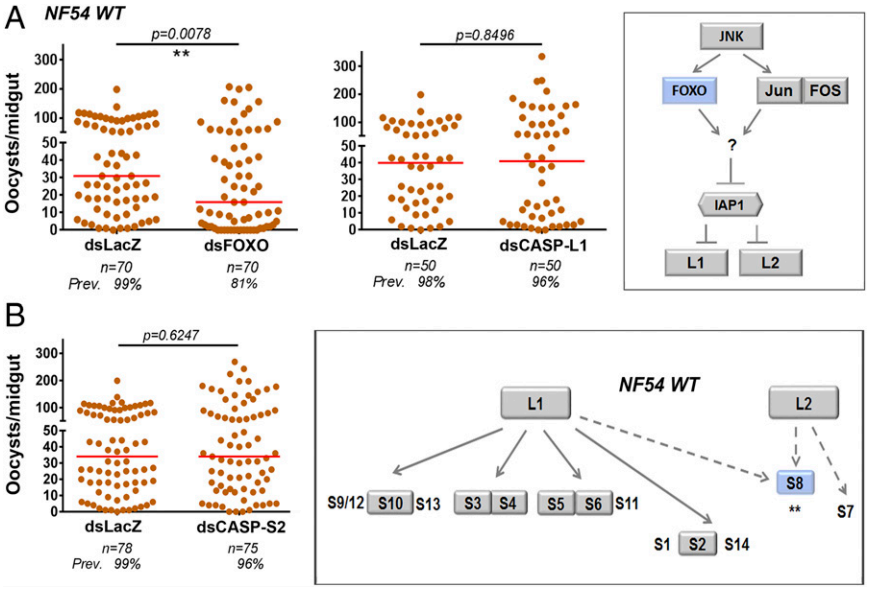

Fig. 4. Effect of silencing caspases on *P. falciparum NF54 WT* infections in *A. gambiae*. (*A*) Effect of silencing FOXO and initiator CASP-L1 or (*B*) silencing CASP-S2 on *NF54 WT* infection. (*Insets*) Geometric shapes represent genes phenotyped using RNAi. Gray color indicates that silencing had no significant effect on infection intensity, red a significant increase in infection, and blue a significant decrease in infection intensity. Asterisks indicate the statistical significance of the differences in infection relative to the dsLacZ controls: $**P < 0.01$. Each phenotype was confirmed with two to three independent experiments.

INAUGURAL ARTICLE
SEE COMMENTARY
MICROBIOLOGY

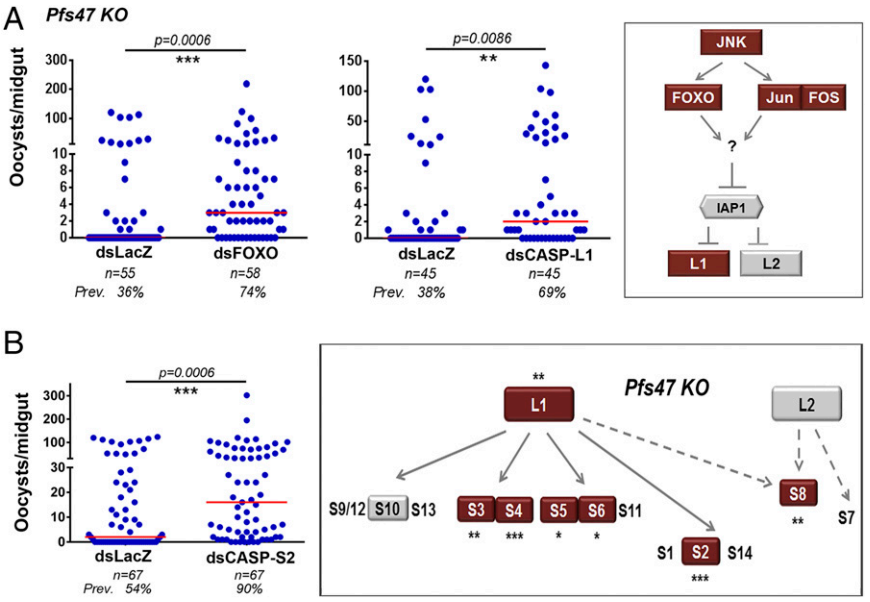

Fig. 5. Effect of silencing caspases on *P. falciparum Pfs47 KO* infections in *A. gambiae*. (*A*) Effect of silencing FOXO and initiator CASP-L1 or (*B*) silencing CASP-S2 on *Pfs47 KO* infection. (*Insets*) Geometric shapes represent genes phenotyped using RNAi. Gray color indicates that silencing had no significant effect on infection intensity and red, a significant increase in infection intensity. Asterisks indicate the statistical significance of the differences in infection relative to the dsLacZ controls: $*P < 0.05$, $**P < 0.01$, $***P < 0.001$. Each phenotype was confirmed with two to three independent experiments.

In contrast, parasites that lack *Pfs47* but are otherwise genetically identical, elicit a very different response when they invade the mosquito midgut. Silencing different components of the JNK pathway greatly enhanced survival of *Pfs47 KO* parasites, indicating that this signaling pathway plays an active role in eliminating these parasites. Collectively, we show that *Pfs47* is able to evade the mosquito immune system by disrupting JNK signaling, and thus preventing the induction of HPX2 and NOX5 and the subsequent midgut nitration response. The parasites that are not nitrated remain undetected by TEP1 and develop into oocysts. However, in the absence of *Pfs47*, the JNK pathway is active, induces HPX2 and NOX5 expression, and a strong nitration response that ultimately results in parasite lysis. We confirmed the previous reports that IMD pathway limits *P. falciparum* infection (30, 31), and found that activation of this pathway is not affected by *Pfs47*.

We also undertook a broad approach to identify novel genes that might be affected by *Pfs47*, by comparing the transcriptional responses of the mosquito midgut to infection with *NF54 WT* and *Pfs47 KO* parasites. At 12 h PF, before parasites invaded the mosquito midgut, some broad differences in the midgut transcriptional responses were already apparent. For example, the number of induced genes in mosquitoes infected with *WT* parasites was 3.5-fold higher than in those infected with *Pfs47 KO*, and many genes were differentially induced or repressed in response to infection with *WT* and *KO* parasites (Fig. 3*A*), indicating that *Pfs47* expression in female gametes, zygotes and immature ookinetes is already affecting the mosquito midgut response to infection. At the time of peak ookinete midgut invasion (26 h PF), drastic differences were also observed. The dramatic number of suppressed genes in response to *Pfs47 KO* parasite invasion (Fig. 3*B*) suggests that midgut cells probably undergo extensive damage, and it is also likely that cells damaged by parasite invasion trigger a response in their neighboring healthy cells, resulting in a global suppression of numerous housekeeping genes. Most genes also had very different transcriptional responses to invasion by *WT* and *KO* parasites at this later time (Fig. 3 and Table S2).

The functional dsRNA-mediated silencing screen identified CASP-S2 as a gene that limits survival of *KO* parasites, but that has no effect on *NF54 WT* parasites expressing *Pfs47*. In addition to the role of JNK signaling in insect immunity, in *Drosophila*, JNK signaling also regulates apoptosis (10) and has also been shown to activate caspases that mediate cell death in human myeloid leukemia cell lines (41). This finding prompted us to explore whether the disruption of JNK signaling by *Pfs47* was affecting the epithelial apoptotic response to *Plasmodium*

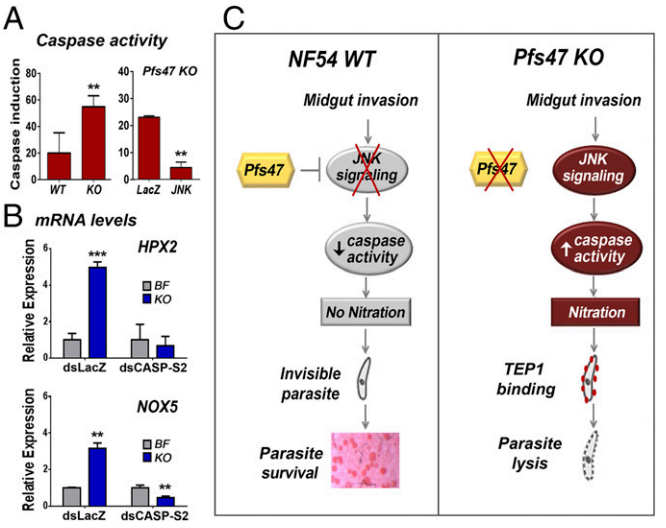

Fig. 6. The JNK pathway regulates epithelial cell death and nitration. (*A*, *Left*) Increase in Caspase-3 activity (AFC fluorescence) in pools of midguts 28 h PF after infection with either *NF54 WT* or *Pfs47 KO* parasites. (*Right*) Effect of silencing LacZ or JNK on induction of midgut caspase activity following *Pfs47 KO* infection, above levels in control females fed on uninfected blood. (*B*) Effect of systemic injection of *dsLacZ* or *dsCASP-S2* on mRNA expression of HPX2 and NOX5 in mosquito midguts bloodfed on uninfected blood (BF) or infected with *Pfs47 KO* parasites (KO). $**P < 0.01$, $***P < 0.001$. (*C*) Summary of the differences in mosquito midgut epithelial responses and infection outcome following infection of *A. gambiae* with *NF54 WT* and *Pfs47 KO* parasites.

invasion. We found that silencing *JNK*, *Jun*, *Fos*, or the initiator caspase CASP-L1 (ortholog of *Drosophila Dredd*) had no effect on *NF54 WT* parasites, but greatly enhanced survival of *Pfs47 KO* parasites. Silencing the effector caspases CASP-S2, -S3, -S4, -S5, and -S6 had no effect in *NF54 WT* parasites, but enhanced infection of the *Pfs47 KO* strain, with CASP-S2 and CASP-S4 having the strongest phenotype. This finding suggests that *Pfs47 KO*-invaded midguts undergo an active cell death response mediated by the induction of FOXO, CASP-L1, and several effector caspases. *Pfs47* has a dramatic effect on JNK signaling and apoptotic responses, as we were unable to detect any effect of silencing the genes involved in these responses, even after enhancing the sensitivity of the dsRNA-silencing screen by lowering the temperature and slowing down the mosquito cellular responses to infection.

However, activation of apoptosis in the *Pfs47 KO* line does not appear to involve IAP1 or CASP-L2. Silencing of IAP1 in *A. aegypti* results in very high mortality (42). We also observed some mortality in *A. gambiae* when we silenced IAP1 but at a lower level (20–30%); however, there was no significant effect on survival of either *WT* or *KO* parasites. It is likely that the *A. gambiae* annotated as IAP1 is not the true ortholog of *Drosophila* IAP1, or that the system is redundant and one of the extra IAP genes present in *A. gambiae* is complementing the function. No direct orthologs of the three *Drosophila* IAP antagonist (*hid, sickle*, *grim*, and *reaper*) genes have been identified in *A. gambiae*.

Interestingly, silencing FOXO and the effector caspase CASP-S8 increases susceptibility to infection with *Pfs47 KO* parasites, but reduces survival of *NF54 WT*, indicating that when *Pfs47* is present, activation of this caspase through FOXO may trigger a pathway of cell death that involves CASP-S8 and is beneficial to the survival of *NF54 WT* parasites. Activation of FOXO has also been shown to decrease mitochondrial and cytoplasmic antioxidants (43), so it is possible that silencing FOXO may reduce midgut oxidative stress by increasing the level of antioxidants, and this would be beneficial to the parasite. Interestingly, activation of the same pathway in the absence of *Pfs47*, when JNK signaling is active, triggers a strong apoptotic response that greatly limits infection. CASP-S10 silencing has no effect on survival of either *NF54 WT* or *Pfs47 KO* parasites, suggesting that it is not a critical mediator of antiplasmodial immunity.

Although, in *Drosophila Dredd* can activate the transcription factor Relish through the IMD pathway (31, 44, 45), the phenotypes we observed when CASP-L1 (*Dredd* ortholog) was silenced do not appear to be due to disruption of IMD signaling, because silencing IMD enhanced infection with *NF54 WT* parasites, whereas silencing CASP-L1 had no effect.

Our studies provide direct evidence of a functional link between JNK signaling, apoptosis, and midgut nitration (Fig. 6*C*). We show that *Pfs47* expression on the surface of *NF54 WT* parasites suppresses JNK signaling, resulting in a silent cell death and very low activation of caspase activity in invaded midguts. In contrast, in the absence of *Pfs47*, epithelial cells induce a strong activation of JNK signaling that activates epithelial caspases, resulting in a strong apoptotic response. Silencing CASP-S2 prevents the induction of these two enzymes that potentiate nitration, allowing the parasites to evade the mosquito immune system and survive.

Collectively, our findings indicate that the presence of the *Pfs47* haplotype present in some African *P. falciparum* strains, such as *NF54*, allows the parasite to evade the mosquito immune system of *A. gambiae* mosquitoes by suppressing JNK-mediated apoptosis and epithelial nitration responses during their transit through the mosquito midgut, making the parasite "invisible" to the mosquito complement-like system.

Materials and Methods

Mosquito Strains. The *A. gambiae* G3 strain was reared under standard laboratory conditions of 27 °C and 80% humidity on a 12-h light/dark cycle. Mosquitoes were maintained on 10% (vol/vol) sucrose solution in water, as previously described (46).

***Plasmodium* Infections.** For *P. falciparum* infections, mosquitoes were artificially infected with mature stage IV and V *P. falciparum NF54* or *NF54-Pfs47KO* gametocyte cultures through a membrane feeder at 37 °C for 30 min. Blood was obtained from Interstate Blood Bank. Mosquitoes were maintained at 26 °C for 8–10 d PF until midguts were dissected and stained with 0.1% mercurochrome and numbers of oocysts were counted by light microscopy.

For temperature-switch experiments, mosquitoes were first fed on an infectious or noninfectious bloodmeal. Six hours later, mosquitoes were transferred to an incubator kept at 22.5 °C. Mosquitoes were maintained in the incubator for ~36 h. A tray with water was kept in the incubator to allow for humidity. After 36 h of being kept at 22.5 °C, mosquitoes were returned back to the insectary with normal temperature of 26 °C.

Microarray Design and Analysis. *A. gambiae* G3 strain of mosquitoes were fed on uninfected human blood or fed on two infected blood alternatives: *NF54 WT* or *Pfs47 KO P. falciparum* strains and maintained at 26 °C. Mosquito midguts were collected in 50 μL RNALater (Ambion) in liquid nitrogen and stored at −70 °C until processed. Three replicates of pools of 25 midguts were collected at 12 and 26 h after blood feeding. A cohort of highly permissive *A. stephensi* mosquitoes was coinfected to confirm the quality of the gametocyte cultures used in every experiment. These mosquitoes were dissected 9–10 d PF to confirm infection by counting oocyst numbers. Total RNA was extracted using a modified RNAeasy Mini Kit (Qiagen) and TRIzol (Invitrogen) and cDNA synthesis was performed using QuantiTect Reverse Transcription Kit (Qiagen). RNA integrity was determined using an Agilent Bioanalyzer and Agilent 6000 nano assay. A reference based design was used to compare all midgut samples to a reference pool of midguts (Fig. S2*B*). The reference pooled sample consisting of mosquitoes infected with *Pfs47 KO* at 12 h and 26 h postinfection was labeled with CY5 and the remaining samples labeled with CY3 using the Quick Amp labeling kit (Agilent). The labeled RNA samples were hybridized to a custom designed 4 × 44 K *A. gambiae* microarray (Agilent). The microarray consisted of 45,220 probes; this includes 22,287 60-mer probes designed against unannotated transcripts using e-Array software (Agilent) with the base composition method. Linker sequences were added to 3′ end of probes to increase probe availability for hybridization. Microarrays were scanned in an Agilent G2505C microarray scanner, and the Agilent feature extraction method was used for image analysis. To define whether normalization between arrays is needed, dye ratio in each array was determined using box plots. The LOWESS method was used for normalization of spot intensities within arrays. The limit of gene expression was determined to be ≥2.0 fold-change (1 in $\log_2$ scale) in comparisons between *NF54/BF* and *Pfs47KO/BF* and statistically significant using a moderated *t* test of $P < 0.05$ in two of three replicates.

qRT-PCR Expression Analysis. Total RNA were isolated from 15 to 20 mosquito midguts using a modified RNAeasy Mini Kit (Qiagen) and TRIzol (Invitrogen) and cDNA synthesis was performed using QuantiTect Reverse Transcription Kit (Qiagen). Gene-expression analysis was measured by SYBR green qRT-PCR (DyNAmo HS; New England Biolabs) in a CFX96 system. Gene expression was assessed using two to three technical replicates and three biological replicates. The ribosomal protein S7 was used as an internal reference to normalize each sample. Fold-change was calculated using the $2^{-\Delta\Delta}$Ct method. The primers used are listed in Table S3.

RNAi Gene Silencing. T7 sequences were added to gene specific primers to generate ~300- to 500-bp PCR-amplified gene fragments using the T7 RNAi Megascript kit (Ambion). dsRNAs were eluted in water and concentrated to 3 μg/μL using a Microcon YM-100 filter (Millipore). Two- to 3-d-old cold-anesthetized female mosquitoes were injected with 69 nL of 3 μg/μL of target dsRNA or control dsLacZ into the thorax using a nano-injector (Nanoject, Drummond) with glass capillary needles 2–3 d before receiving a *Plasmodium*-infected bloodmeal. Silencing efficiency was measured 2–3 d after injection by qRT-PCR with the *A. gambiae* ribosomal S7 gene as an internal control for normalization. Silencing efficiency was assessed by qRT-PCR.

Caspase Activity Assays. Mosquitoes were fed with *Plasmodium*-infected bloodmeal and caspase-3 activity was measured in mosquito midguts 28 h postinfection after mosquitoes were kept under the temperature-switch protocol as described above. Three pools of five midguts per group were dissected and the blood bolus was removed. Midguts were collected in 50 μL PBS and caspase-3 activity assays were performed according to manufacturer's instructions (Biovision). Briefly, midguts were homogenized, centrifuged, and cell lysis buffer was added. The supernatant was added to a reaction buffer with 1 M DTT, and placed on ice for 10 min, after which 20 μL of the solution was added to a plate and DEVD-AFC caspase-3 fluorometric substrate was subsequently added and left to incubate in the dark for 2 h at 37 °C. Fluorescence readings were taken at 400-nm excitation and 505-nm emission and the control readings were subtracted for background.

Statistical Analysis. All statistical analyses were performed using GraphPad Prism 6 software (GraphPad Software). Gene-expression data were analyzed using Student's *t* test on mean value of all independent experiments. Infection intensity of oocysts was compared with each other using Mann–Whitney tests and infection prevalence were compared using χ^2 tests with Yates correction. Caspase activity levels were compared using Student's *t* test.

ACKNOWLEDGMENTS. We thank Andre Laughinghouse and Kevin Lee for insectary support; Jose Luis Ramirez, Nitin Kamath, Rebecca Greene, Alejandro Padron, Ashley Haile, and Noelle Pavlovic for experimental assistance; and Timothy Myers, Qin Su, and the National Institute of Allergy and Infectious Diseases Genomic Technologies Section for microarray hybridization and scanning. This work was supported by the Intramural Research Program of the Division of Intramural Research, National Institute of Allergy and Infectious Diseases, National Institutes of Health.

1. WHO (2013) *World Malaria Report* (World Health Organization, Geneva).
2. Han YS, Barillas-Mury C (2002) Implications of Time Bomb model of ookinete invasion of midgut cells. *Insect Biochem Mol Biol* 32(10):1311–1316.
3. Luckhart S, Vodovotz Y, Cui L, Rosenberg R (1998) The mosquito *Anopheles stephensi* limits malaria parasite development with inducible synthesis of nitric oxide. *Proc Natl Acad Sci USA* 95(10):5700–5705.
4. Han YS, Thompson J, Kafatos FC, Barillas-Mury C (2000) Molecular interactions between *Anopheles stephensi* midgut cells and *Plasmodium berghei*: The Time Bomb theory of ookinete invasion of mosquitoes. *EMBO J* 19(22):6030–6040.
5. Oliveira GdeA, Lieberman J, Barillas-Mury C (2012) Epithelial nitration by a peroxidase/NOX5 system mediates mosquito antiplasmodial immunity. *Science* 335(6070): 856–859.
6. Blandin S, et al. (2004) Complement-like protein TEP1 is a determinant of vectorial capacity in the malaria vector *Anopheles gambiae*. *Cell* 116(5):661–670.
7. Kumar S, Gupta L, Han YS, Barillas-Mury C (2004) Inducible peroxidases mediate nitration of *Anopheles* midgut cells undergoing apoptosis in response to *Plasmodium* invasion. *J Biol Chem* 279(51):53475–53482.
8. Garver LS, de Almeida Oliveira G, Barillas-Mury C (2013) The JNK pathway is a key mediator of *Anopheles gambiae* antiplasmodial immunity. *PLoS Pathog* 9(9):e1003622.
9. Sluss HK, et al. (1996) A JNK signal transduction pathway that mediates morphogenesis and an immune response in *Drosophila*. *Genes Dev* 10(21):2745–2758.
10. Kockel L, Homsy JG, Bohmann D (2001) *Drosophila* AP-1: Lessons from an invertebrate. *Oncogene* 20(19):2347–2364.
11. Martín-Blanco E, et al. (1998) *puckered* encodes a phosphatase that mediates a feedback loop regulating JNK activity during dorsal closure in *Drosophila*. *Genes Dev* 12(4):557–570.
12. Whitmarsh AJ (2006) The JIP family of MAPK scaffold proteins. *Biochem Soc Trans* 34(Pt 5):828–832.
13. Vaishnav M, MacFarlane M, Dickens M (2011) Disassembly of the JIP1/JNK molecular scaffold by caspase-3–mediated cleavage of JIP1 during apoptosis. *Exp Cell Res* 317(7): 1028–1039.
14. Bonny C, Nicod P, Waeber G (1998) IB1, a JIP-1–related nuclear protein present in insulin-secreting cells. *J Biol Chem* 273(4):1843–1846.
15. Negri S, et al. (2000) cDNA cloning and mapping of a novel islet-brain/JNK-interacting protein. *Genomics* 64(3):324–330.
16. Kelkar N, Gupta S, Dickens M, Davis RJ (2000) Interaction of a mitogen-activated protein kinase signaling module with the neuronal protein JIP3. *Mol Cell Biol* 20(3): 1030–1043.
17. Ito M, et al. (1999) JSAP1, a novel jun N-terminal protein kinase (JNK)-binding protein that functions as a Scaffold factor in the JNK signaling pathway. *Mol Cell Biol* 19(11): 7539–7548.
18. Kelkar N, Standen CL, Davis RJ (2005) Role of the JIP4 scaffold protein in the regulation of mitogen-activated protein kinase signaling pathways. *Mol Cell Biol* 25(7): 2733–2743.
19. Luo X, Puig O, Hyun J, Bohmann D, Jasper H (2007) Foxo and Fos regulate the decision between cell death and survival in response to UV irradiation. *EMBO J* 26(2):380–390.
20. Greer EL, Brunet A (2005) FOXO transcription factors at the interface between longevity and tumor suppression. *Oncogene* 24(50):7410–7425.
21. Drexler AL, et al. (2014) Human IGF1 regulates midgut oxidative stress and epithelial homeostasis to balance lifespan and *Plasmodium falciparum* resistance in *Anopheles stephensi*. *PLoS Pathog* 10(6):e1004231.
22. Zhou L, et al. (2005) Michelob_x is the missing inhibitor of apoptosis protein antagonist in mosquito genomes. *EMBO Rep* 6(8):769–774.
23. Wilson R, et al. (2002) The DIAP1 RING finger mediates ubiquitination of *Dronc* and is indispensable for regulating apoptosis. *Nat Cell Biol* 4(6):445–450.
24. Shlevkov E, Morata G (2012) A *dp53*/JNK-dependant feedback amplification loop is essential for the apoptotic response to stress in *Drosophila*. *Cell Death Differ* 19(3): 451–460.
25. Kumar S (2007) Caspase function in programmed cell death. *Cell Death Differ* 14(1): 32–43.
26. Cooper DM, Granville DJ, Lowenberger C (2009) The insect caspases. *Apoptosis* 14(3): 247–256.
27. Thornberry NA, Lazebnik Y (1998) Caspases: Enemies within. *Science* 281(5381): 1312–1316.
28. Frolet C, Thoma M, Blandin S, Hoffmann JA, Levashina EA (2006) Boosting NF-kappaB-dependent basal immunity of *Anopheles gambiae* aborts development of *Plasmodium berghei*. *Immunity* 25(4):677–685.
29. Meister S, et al. (2005) Immune signaling pathways regulating bacterial and malaria parasite infection of the mosquito *Anopheles gambiae*. *Proc Natl Acad Sci USA* 102(32):11420–11425.
30. Garver LS, Dong Y, Dimopoulos G (2009) Caspar controls resistance to *Plasmodium falciparum* in diverse anopheline species. *PLoS Pathog* 5(3):e1000335.
31. Garver LS, et al. (2012) *Anopheles* IMD pathway factors and effectors in infection intensity-dependent anti-*Plasmodium* action. *PLoS Pathog* 8(6):e1002737.
32. Gupta L, et al. (2009) The STAT pathway mediates late-phase immunity against *Plasmodium* in the mosquito *Anopheles gambiae*. *Cell Host Microbe* 5(5):498–507.
33. Molina-Cruz A, et al. (2013) The human malaria parasite *Pfs47* gene mediates evasion of the mosquito immune system. *Science* 340(6135):984–987.
34. Dong Y, et al. (2011) Engineered *Anopheles* immunity to *Plasmodium* infection. *PLoS Pathog* 7(12):e1002458.
35. Silverman N, et al. (2003) Immune activation of NF-kappaB and JNK requires *Drosophila* TAK1. *J Biol Chem* 278(49):48928–48934.
36. Delaney JR, et al. (2006) Cooperative control of *Drosophila* immune responses by the JNK and NF-kappaB signaling pathways. *EMBO J* 25(13):3068–3077.
37. Leulier F, Lhocine N, Lemaitre B, Meier P (2006) The *Drosophila* inhibitor of apoptosis protein DIAP2 functions in innate immunity and is essential to resist gram-negative bacterial infection. *Mol Cell Biol* 26(21):7821–7831.
38. Tsuda M, Langmann C, Harden N, Aigaki T (2005) The RING-finger scaffold protein Plenty of SH3s targets TAK1 to control immunity signalling in *Drosophila*. *EMBO Rep* 6(11):1082–1087.
39. An C, et al. (2012) Biochemical characterization of *Anopheles gambiae* SRPN6, a malaria parasite invasion marker in mosquitoes. *PLoS ONE* 7(11):e48689.
40. Liu Q, Clem RJ (2011) Defining the core apoptosis pathway in the mosquito disease vector *Aedes aegypti*: The roles of *iap1*, *ark*, *dronc*, and effector caspases. *Apoptosis* 16(2):105–113.
41. Seimiya H, Mashima T, Toho M, Tsuruo T (1997) c-Jun NH_2-terminal kinase-mediated activation of interleukin-1β converting enzyme/CED-3–like protease during anticancer drug-induced apoptosis. *J Biol Chem* 272(7):4631–4636.
42. Ocampo CB, et al. (2013) Differential expression of apoptosis related genes in selected strains of *Aedes aegypti* with different susceptibilities to dengue virus. *PLoS ONE* 8(4): e61187.
43. Luckhart S, et al. (2013) Sustained activation of Akt elicits mitochondrial dysfunction to block *Plasmodium falciparum* infection in the mosquito host. *PLoS Pathog* 9(2): e1003180.
44. Stöven S, Ando I, Kadalayil L, Engström Y, Hultmark D (2000) Activation of the *Drosophila* NF-kappaB factor Relish by rapid endoproteolytic cleavage. *EMBO Rep* 1(4): 347–352.
45. Stoven S, et al. (2003) Caspase-mediated processing of the *Drosophila* NF-kappaB factor Relish. *Proc Natl Acad Sci USA* 100(10):5991–5996.
46. Benedict MQ (1997) Care and maintenance of anopheline mosquito colonies. *The Molecular Biology of Disease Vectors: A Methods Manual*, eds Crampton JM, Beard CB, Louis C (Champman & Hall, London), pp 3–12.